³¹P NMR Chemical Shift Tensors: Windows into Ruthenium–Phosphinidene Complex Electronic Structures

Wesley J. Transue,† Yizhe Dai,‡ Martin-Louis Y. Riu,† Gang Wu,‡ and Christopher C. Cummins*,†

 $\label{eq:continuity} \begin{array}{l} \dagger Department\ of\ Chemistry,\ Massachusetts\ Institute\ of\ Technology,\ Cambridge,\ MA\ 02139,\ USA\\ \ddagger Department\ of\ Chemistry,\ Queen's\ University,\ Kingston,\ ON\ K7L3N6,\ Canada \end{array}$

Received June 11, 2021; E-mail: ccummins@mit.edu

Abstract: A series of octamethylcalix[4]pyrrole ruthenium phosphinidene complexes (Na₂[1=PR]) can be accessed by phosphinidene transfer from corresponding RPA ($\mathbf{A} = C_{14}H_{10}$, anthracene) compounds ($R = {}^{t}Bu$, ${}^{i}Pr$, OEt, NH_2 , NMe_2 , NEt₂, NⁱPr₂, NA, dimethylpiperidino). Isolation of the tertbutyl and dimethylamino derivatives allowed comparative studies of their ³¹P nuclear shielding tensors by magic anglespinning (MAS) solid-state nuclear magnetic resonance (NMR) spectroscopy. Density functional theory (DFT) and natural chemical shielding (NCS) analyses reveal the relationship between the ³¹P chemical shift tensor and the local ruthenium-phosphorus electronic structure. The general trend observed in ³¹P isotropic chemical shifts for the ruthenium phosphinidene complexes was controlled by the degree of deshielding in the δ_{11} principal tensor component, which can be linked to the $\sigma_{\rm RuP}/\pi_{\rm RuP}^*$ energy gap. A " δ_{22} - δ_{33} crossover" effect for R = ^tBu was also observed, caused by different degrees of deshielding associated with polarizations of the $\sigma_{\rm PR}$ and $\sigma_{\rm PR}^*$ natural bond orbitals (NBOs).

Chemical shift tensors inform us about electronic structure through both their magnitudes and anisotropies, a fact readily seen through Ramsey's classic perturbational treatment of nuclear shielding. This link between solid-state nuclear magnetic resonance (SSNMR) spectroscopy and electronic structure has proven especially useful in investigations of transition metal–ligand multiple bonds, $^{2-5}$ including our own studies of $\rm Pn\equiv Mo~(Pn=^{15}N,~^{31}P)^{6,7}$ centers. Particularly sophisticated have been the studies from the Copéret lab using $^{13}\rm C$ magic-angle spinning (MAS) SSNMR spectroscopy as a central tool in the design and understanding of d^0 olefin metathesis catalysts. $^{8-11}$ While there have been studies of ways $^{31}\rm P$ chemical shifts may inform electronic structure of transition metal complexes, 12,13 the field remains relatively unexplored. Against this backdrop, we have sought to expand the understanding of metal–phosphinidene bonding through $^{31}\rm P~MAS~SSNMR~studies$.

Our recent work on phosphinidene transfer from dibenzo-7-phosphanorbornadiene RPA compounds ($\mathbf{A} = C_{14}H_{10}$ or anthracene) has positioned us well to explore [RP] unit delivery to a metal center. We now report facile phosphinidene transfer from a series of RPA compounds to a ruthenium(II) calix[4]pyrrole ("porphyrinogen") complex Na₂(DME)₆[1] (Fig. 1). ^{14,15} The electronic structure of the resulting Ru=P bond is strongly influenced by the substituent, an effect we have characterized through ³¹P MAS SSNMR spectroscopy. The chemical shift tensor is shown to be a direct experimental handle on the $\sigma_{\text{Ru}=P}/\pi_{\text{Ru}=P}^*$ energy gap and its orienta-

tion on the nature of the phosphorus–substituent σ_{PR} bond. Density functional theory (DFT) calculations and natural chemical shielding (NCS) analysis were central in uncovering these connections.

First investigated by Floriani et al. in 2001, ^{14,15} the ruthenium(II) platform [1]²⁻ has been reported to support a variety of ruthenium-main group multiple bonds. 14-16 Our studies began by interrogating the reaction between $Na_2(DME)_6[1]$ and tBuPA by NMR spectroscopy in THF d_8 . Although originally reported to have a ¹H NMR spectrum consistent with [1]²⁻ being a closed-shell complex, ¹⁷ we have found THF- d_8 solutions of Na₂(DME)₆[1] to exhibit a single paramagnetically shifted resonance at $^{1}{\rm H}$ δ –28.3 (s, 8H) ppm, indicating that $[1]^{2-}$ is likely of intermediate spin S=1, as is typical for square-planar d^6 ruthenium(II) complexes. ^{18–20} Monitoring the reaction between Na₂(DME)₆[1] and ${}^{t}\mathrm{BuP}\mathbf{A}^{21}$ over 24 h showed gradual loss of the ${}^{1}\mathrm{H}$ δ -28.3 ppm resonance and growth of a new resonance in the $^{31}\mathrm{P}\{^{1}\mathrm{H}\}$ NMR spectrum at δ 1047 ppm, characteristic of a bent phosphinidene. 22 This change was accompanied by a dramatic color change from orange-red to purple.

The reaction was relatively slow even at elevated temperatures $(k = 8.7(4) \times 10^{-4} \text{ M}^{-1} \text{ s}^{-1}, 80 \text{ °C}, \text{THF-}d_8;$ see SI §S1.7), but could be accelerated by addition of excess ${}^t\text{BuPA}$. Full conversion to this new species was achieved by heating Na₂(DME)₆[1] with 3 equiv ${}^t\text{BuPA}$ (80 °C, 18 h, THF), and the product crystallized from hot dioxane solution to yield Na₂(dioxane)₅[1=P ${}^t\text{Bu}$] (33% isol.) as deep purple blocks. Characterization by an X-ray diffraction (XRD) study revealed a Ru–P–C angle of 121.57(3)° and a

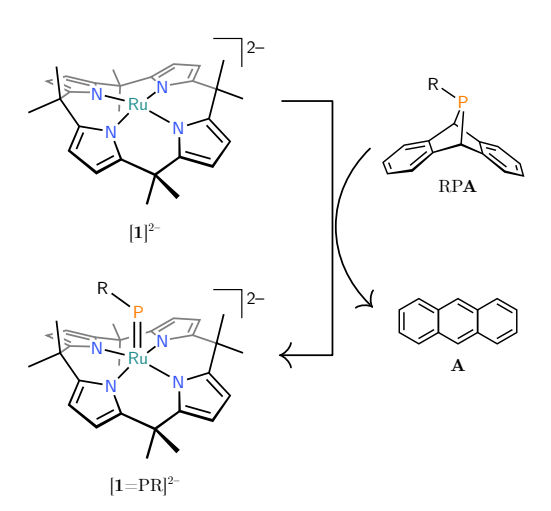


Figure 1. The ruthenium(II) complex $\mathrm{Na_2(DME)_6[1]}$ accepts phosphinidene fragments from a series of RPA compounds.

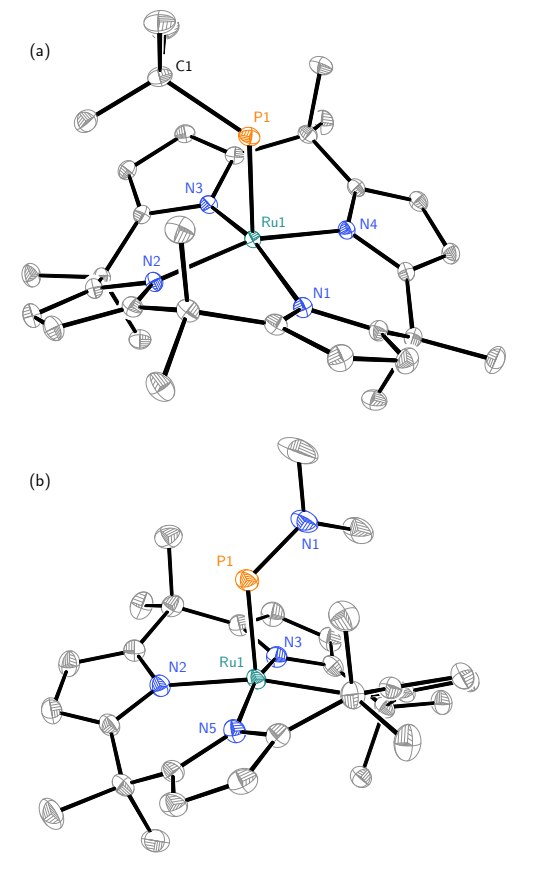


Figure 2. X-ray crystallographic structures (see SI \S S2) of (a) Na₂(dioxane)₅[1=P^tBu] and (b) Na₂(dioxane)₄[1=PNMe₂] with sodium, dioxane, and hydrogen centers omitted for clarity. (a) Selected interatomic distances (Å) and angles (°): average Ru–N 2.0591(8), Ru–P 2.1156(3), P–C 1.8981(11); Ru–P–C 121.57(3). (b) Selected interatomic distances and angles: average Ru–N 2.053(3), Ru–P 2.0829(8), P–N 1.666(3); Ru–P–N 121.05(11).

Ru=P bond length of 2.1156(3) Å (Fig. 2a), shorter than any ruthenium–phosphinidene bond currently catalogued in the Cambridge Structural Database (CSD). 23 It is also slightly shorter than the sum of the two double-bond covalent radii (2.16 Å). 24

Similar studies combining Me_2NPA^{25} and $Na_2(DME)_6[1]$ provided analogous formation of dark purple $[1=PNMe_2]^{2-}$ (18 h, 22 °C) by ^{31}P NMR spectroscopy (δ 791 ppm). The product could be isolated as a $Na_2(dioxane)_4[1=PNMe_2]$ salt following recrystallization from hot dioxane (62% isol. yield). Structural parameters from an XRD study (Fig. 2b) are similar to those of $Na_2(dioxane)_5[1=P^tBu]$ with a slightly shorter Ru=P bond length of 2.0829(8) Å and a Ru-P-N angle of $121.05(11)^\circ$.

The ruthenium calix[4]pyrrole platform proved quite versatile in phosphinidene complex formation. Treatment with a medley of RPA compounds showed successful formation of the anticipated $[1=PR]^{2-}$ species in situ by ³¹P NMR spectroscopy, resonating over a wide (~300 ppm) range of chemical shifts (Fig. 3). The only exceptions were ClPA ^{25,26} and HPA, ²⁷ which yielded complicated mixtures of products, and $(Me_3Si)_2NPA$, ²¹ which we presume was too sterically encumbered to react. Additionally, extended heating of Na₂(DME)₆[1] with (tBuP)₃ ²⁸ (48 h, 80 °C) did not lead to observation of $[1=P^tBu]^{2-}$ in the ³¹P NMR spectrum, indicating that RPA compounds are superior phosphinidene group transfer reagents for this transformation.

The wide range of chemical shifts demonstrated high sensitivity of the resonance to the electronic structure of the Ru=PR center. Collection of $^{31}{\rm P}$ MAS SSNMR spectra of Na₂(dioxane)₅[1=P^tBu] and Na₂(dioxane)₄[1=PNMe₂] added insight into the nature of the phosphorus chemical shift tensors (Fig. 4a–b). The large spans of the tensors ($\Omega=\delta_{11}-\delta_{33}=1852$ and 1740, respectively) are characteristic of multiply bonded phosphorus centers, 7,29 and their highly negative skews ($\kappa=3(\delta_{22}-\delta_{\rm iso})/\Omega=-0.82$ and -0.55, respectively) indicate a single highly-deshielded direction as expected of a double bond. $^{30-33}$ Interestingly, the larger solution $^{31}{\rm P}$ chemical shift $\delta_{\rm sol}$ of Na₂(dioxane)₅[1=P^tBu] than that of Na₂(dioxane)₄[1=PNMe₂] was reflected in all three directions of the chemical shift tensors obtained by simulation of the $^{31}{\rm P}$ MAS SSNMR spectra.

Interpretation of these tensors was assisted by density functional theory (DFT) and the natural chemical shielding (NCS)³⁴ analytical subroutine of the natural bond orbital (NBO) program (see SI §S3). 35 Nuclear shielding calculations yielded the tensors shown in Fig. 4c-e upon varying the substituent from tert-butyl to dimethylamino and methoxy. The axis of strongest deshielding (δ_{11}) uniformly resides in the Ru-P-R plane and is approximately perpendicular to the Ru-P bond, a consequence of the strong paramagnetic deshielding induced by nucleus-orbit coupling between the $\sigma_{\rm Ru=P}$ and $\pi_{\rm Ru=P}^*$ NBOs. This can be visualized as a 90° rotation of the σ bond along the δ_{11} principal axis providing significant orbital overlap with the π^* orbital. Such behavior mirrors that of $^{13}\mathrm{C}$ NMR chemical shifts for d^0 olefin metathesis catalysts. ⁸ The δ_{11} contributions from the σ/π^* interaction were quantified by NCS analysis to be 1987 ppm (t Bu), 1545 ppm (NMe₂), and 1740 ppm (OMe), giving a trend that matches the solution δ_{iso} values.

Ramsey's theory of nuclear shielding can be used for a qualitative explanation of this phenomenon. Ramsey's perturbative treatment relates paramagnetic deshielding to the sum-over-states¹

$$\delta_{uv}^{\text{para}} \propto \sum_{k>0} \frac{\text{Re}\left[\langle 0|L_u|k\rangle\langle k|L_{\alpha,v}r_{\alpha}^{-3}|0\rangle\right]}{E_0 - E_k}.$$
 (1)

Here, α is the nucleus of interest (the phosphorus-31 center), u/v index the Cartesian directions (xyz), $|0\rangle$ is the ground state, $|k\rangle$ indexes all excited states, E_X is the energy of state X, Re indicates the real part of a complex number, L_u is

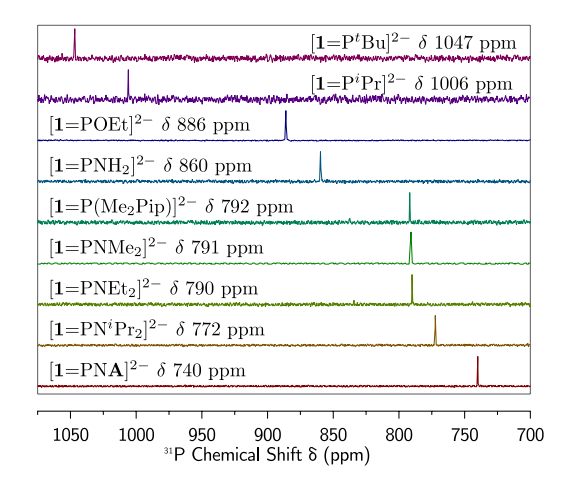


Figure 3. ³¹P NMR spectra of several phosphinidene complexes $[1=PR]^{2-}$ (Me₂Pip = cis-2,6-dimethylpiperidino).

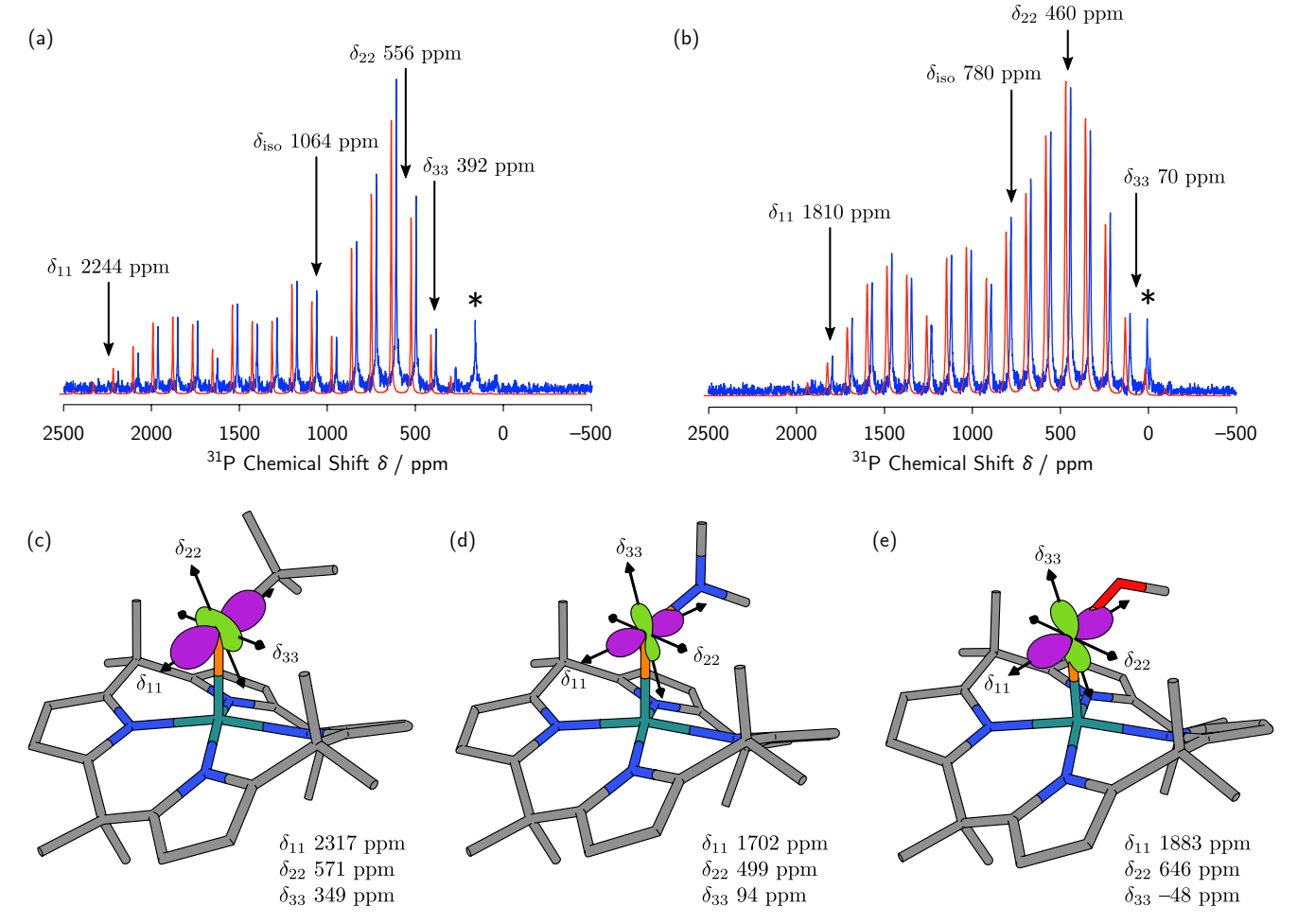


Figure 4. (a, b) Experimental (blue) and simulated (red) ^{31}P MAS SSNMR (16.4 T, 85% aq. H_3PO_4 δ 0 ppm) spectra of (a) $Na_2(dioxane)_5[1=P^tBu]$ and (b) $Na_2(dioxane)_5[1=PNMe_2]$. Simulations are deliberately offset downfield for easy visual inspection. Minor impurities are marked with an asterisk (*). (c, d, e) Plots of the anisotropic components of the calculated chemical shift tensors for (c) $Na_2(OMe_2)_5[1=P^tBu]$, (d) $Na_2(OMe_2)_5[1=PNMe_2]$, and (e) $Na_2(OMe_2)_5[1=POMe]$ as $\vec{r}(\delta-\frac{1}{3}\text{Tr }\delta)\vec{r}$ for $r=(\sin\theta\cos\phi,\sin\theta\sin\phi,\cos\theta)$. Principal axes are illustrated with arrows; purple lobes indicate downfield shift relative to δ_{iso} and green indicate upfield. Sodium atoms, hydrogen atoms, and molecules of solvation are omitted for clarity. Note the directions of δ_{22}/δ_{33} are inverted in (c) versus (d, e).

the u component of the angular momentum operator, r_{α} is the distance from nucleus α , and $L_{\alpha,v}$ is the v component of the angular momentum operator relative to nucleus α . The low-lying $\pi_{\text{Ru}=P}^*$ orbital provides a small E_0-E_k denominator leading to strong deshielding. The δ_{11} shift is thus controlled by the energy of the π^* orbital, which is in turn controlled by the nature of the phosphinidene substituent. Stronger donors should destabilize the $\pi_{\text{Ru}=P}^*$ orbital, so the δ_{11} shift is a direct experimental readout of π donicity. Indeed, the tert-butyl derivative has the most downfield shift of the three, the strong π -donor dimethylamino derivative the most upfield, and the weaker π -donor methoxy derivative is intermediate.

A second interesting difference between the tensors is readily observed in Fig. 4c–e, which shows δ_{22} and δ_{33} are reversed in the *tert*-butyl derivative. ^{37,38} NCS calculations clearly reveal that the orientation of the tensor is dictated by a balance of influences from the σ_{RuP} and σ_{PR} NBOs (SI Table S2). The σ_{PR} NBO contributes to deshielding along the Ru–P bond through coupling to the π_{RuP}^* antibonding NBO, and the σ_{RuP} NBO contributes perpendicular to the Ru–P–R plane through coupling to the σ_{RuP}^* antibond. Both influences seem to reflect the polarization of the phosphorus-substituent interaction (Table 1). As the electronegativity

Table 1. Percent Phosphorus Character of NBOs

NBO	Substituent		
TIBO	$^{t}\mathrm{Bu}$	NMe_2	OMe
$\sigma_{ m RuP}$	56%	47%	51%
σ^*_{RuP}	44%	53%	49%
π_{RuP}	67%	72%	68%
π^*_{RuP}	33%	28%	32%
σ_{PR}	37%	24%	19%
σ_{PR}^*	63%	76%	81%

of the substituent increases, the phosphorus character of the $\sigma_{\rm PR}$ NBO decreases and that of $\sigma_{\rm PR}^*$ correspondingly increases. The $^{31}{\rm P}$ deshielding influence of the NBO parallels its phosphorus character, meaning the percent phosphorus character should correlate with the NBO influence. Indeed, this is seen for both the $\sigma_{\rm PR}$ contribution along the Ru–P bond ($^t{\rm Bu}$ 1166 ppm, $\sigma_{\rm PR}$ 37% P; NMe₂ 497 ppm, $\sigma_{\rm PR}$ 24% P; OMe 405 ppm, $\sigma_{\rm PR}$ 19% P) and the $\sigma_{\rm RuP}$ contribution perpendicular to the Ru–P–R plane ($^t{\rm Bu}$ 434 ppm, $\sigma_{\rm PR}^*$ 63% P; NMe₂ 559 ppm, $\sigma_{\rm PR}^*$ 76% P; OMe 693 ppm, $\sigma_{\rm PR}^*$ 81% P). In this way, the orientation of the δ_{22} and δ_{33} axes is an

experimental reflection of the polarization of the P-R bond.

Influences on the ³¹P chemical shift tensor are undoubtedly multifaceted; however, the wide array of derivatives available from $Na_2(DME)_6[1]$ has allowed us to map out several of the strongest factors. In this way, ³¹P MAS SS-NMR spectroscopy makes experimentally accessible the local electronic structure of the Ru=PR moiety. Leverage of analogous information in d^0 olefin metathesis catalysts has been a major influence in the design of early transition metal alkylidene catalysts, $^{8-11}$ hinting that $^{31}{\rm P}$ MAS SSNMR spectroscopy may be a boon to similar advances in phosphinidene chemistry. Such analogies with metathesis and cyclopropanation catalysts were an early motive in the preparation of the $[1=PR]^{2-}$ complexes, as we have recently begun to investigate catalytic "phosphiranation" reactions.³⁹ We plan to use SSNMR to guide the search for further phosphinidene transfer catalysts.

Acknowledgement This material is based on research supported by the National Science Foundation under CHE-1955612. GW thanks NSERC of Canada for funding.

Notes. The authors declare no competing financial inter-

Supporting Information Available

Full synthetic and computational details, including preparative procedures, spectroscopic data, and crystallographic data for characterization of compounds, are in the supplementary materials.

References

- (1) Flygare, W. H. Magnetic interactions in molecules and an analysis of molecular electronic charge distribution from magnetic
- parameters. Chem. Rev. 1974, 74, 653–687. Greco, J. B.; Peters, J. C.; Baker, T. A.; Davis, W. M.; Cummins, C. C.; Wu, G. Atomic Carbon as a Terminal Ligand: Studies of a Carbidomolybdenum Anion Featuring Solid-State ¹³C NMR Data and Proton-Transfer Self-Exchange Kinetics. J. Am. Chem. Soc. 2001, 123, 5003-5013.
- Zhao, G.; Basuli, F.; Kilgore, U. J.; Fan, H.; Aneetha, H.; Huffman, J. C.; Wu, G.; Mindiola, D. J. Neutral and Zwitterionic Low-Coordinate Titanium Complexes Bearing the Terminal Phosphinidene Functionality. Structural, Spectroscopic, Theoretical, and Catalytic Studies Addressing the Ti-P Multi-
- ple Bond. J. Am. Chem. Soc. 2006, 128, 13575–13585.
 Thompson, R.; Chen, C.-H.; Pink, M.; Wu, G.; Mindiola, D. J.
 A Nitrido Salt Reagent of Titanium. J. Am. Chem. Soc. 2014, 136, 8197-8200.
- Zhu, J.; Kurahashi, T.; Fujii, H.; Wu, G. Solid-state ¹⁷O NMR and computational studies of terminal transition metal oxo compounds. Chem. Sci. **2012**, 3, 391–397.
- Sceats, E. L.; Figueroa, J. S.; Cummins, C. C.; Loening, N. M.; Van der Wel, P.; Griffin, R. G. Complexes obtained by electrophilic attack on a dinitrogen-derived terminal molybdenum nitride: electronic structure analysis by solid state CP/MAS ¹⁵N NMR in combination with DFT calculations. Polyhedron **2004**, 23, 2751–2768.
- 2004, 23, 2131–2108. Wu, G.; Rovnyak, D.; Johnson, M. J. A.; Zanetti, N. C.; Musaev, D. G.; Morokuma, K.; Schrock, R. R.; Griffin, R. G.; Cummins, C. C. Unusual ³¹P Chemical Shielding Tensors in Terminal Phosphido Complexes Containing a Phosphorus–Metal Triple Bond. J. Am. Chem. Soc. 1996, 118, 10654– 10655.
- Halbert, S.; Copéret, C.; Raynaud, C.; Eisenstein, O. Elucidating the Link between NMR Chemical Shifts and Electronic Structure in d^0 Olefin Metathesis Catalysts. J. Am. Chem. Soc. **2016**, *138*, 2261–2272.
- Gordon, C. P.; Yamamoto, K.; Liao, W.-C.; Allouche, F.; Andersen, R. A.; Copéret, C.; Raynaud, C.; Eisenstein, O. Metathesis Activity Encoded in the Metallacyclobutane Carbon-13 NMR Chemical Shift Tensors. ACS Cent. Sci. 2017, 3, 759-768.

- (10) Gordon, C. P.; Culver, D. B.; Conley, M. P.; Eisenstein, O.; Andersen, R. A.; Copéret, C. π-Bond Character in Metal-Alkyl Compounds for C-H Activation: How, When, and Why? J. Am. Chem. Soc. 2019, 141, 648-656.
- (11) Gordon, C. P.; Copéret, C. Metal Alkyls with Alkylidynic Metal-Carbon Bond Character: Key Electronic Structures in Alkane Metathesis Precatalysts. Angew. Chem. Int. Ed. 2020, 59,
- (12) Raynaud, C.; Norbert-Agaisse, E.; James, B. R.; Eisenstein, O. ³¹P Chemical Shifts in Ru(II) Phosphine Complexes. A Computational Study of the Influence of the Coordination Sphere. Inorg. Chem. 2020, 59, 17038–17048.
- Azofra, L. M.; Vummaleti, S. V. C.; Zhang, Z.; Poater, A.; Cavallo, L. σ/π Plasticity of NHCs on the Ruthenium-Phosphine and Ruthenium=Ylidene Bonds in Olefin Metathesis Catalysts.

 Organometallics 2020, 39, 3972-3982.

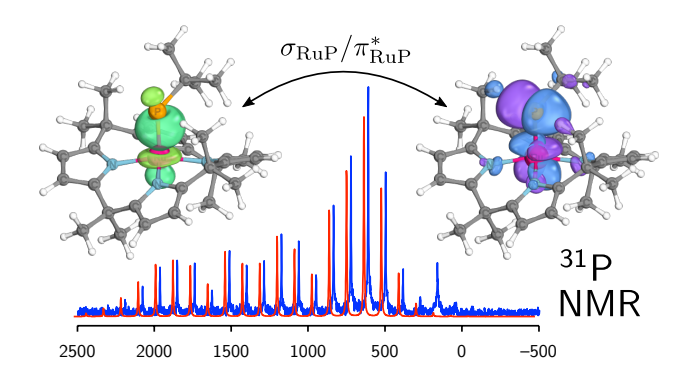
 (14) Bonomo, L.; Stern, C.; Solari, E.; Scopelliti, R.; Flori-
- ani, C. Acetylenes Rearranging on Ruthenium-Porphyrinogen and Leading to Vinylidene and Carbene Functionalities. *Angew*. Chem. Int. Ed. 2001, 40, 1449–1452.
- (15) Bonomo, L.; Solari, E.; Scopelliti, R.; Floriani, C. Ruthenium Nitrides: Redox Chemistry and Photolability of the Ru–Nitrido
- Group. Angew. Chem. Int. Ed. 2001, 40, 2529-2531.

 (16) Joost, M.; Nava, M.; Transue, W. J.; Martin-Drumel, M.-A.; McCarthy, M. C.; Patterson, D.; Cummins, C. C. Sulfur monoxide thermal release from an anthracene-based precursor, spectroscopic identification, and transfer reactivity. Proc. Natl. Acad. Sci. 2018, 115, 5866–5871.
- (17) Floriani's reported NMR experiments were conducted with a DMSO- d_6 solvent. We have found this to result in a diamagnetic octahedral complex, which we have characterized crystallographically (see SI).
- Watson, L. A.; Ozerov, O. V.; Pink, M.; Caulton, K. G. Four-Coordinate, Planar Ru(II). A Triplet State as a Response to a 14-Valence Electron Configuration. J. Am. Chem. Soc. 2003,
- Askevold, B.; Khusniyarov, M. M.; Herdtweck, E.; Meyer, K.; Schneider, S. A Square-Planar Ruthenium(II) Complex with a Low-Spin Configuration. Angew. Chem. Int. Ed. 2010, 49, 7566–7569.
- Askevold, B.; Khusniyarov, M. M.; Kroener, W.; Gieb, K.; Müller, P.; Herdtweck, E.; Heinemann, F. W.; Diefenbach, M.; Holthausen, M. C.; Vieru, V.; Chibotaru, L. F.; Schneider, S. Square-Planar Ruthenium(II) Complexes: Control of Spin State by Pincer Ligand Functionalization. Chem. Eur. J. 2015, 21, 579–589.
- (21) Velian, A.; Cummins, C. C. Facile Synthesis of Dibenzo- $7\lambda^3$ -phosphanorbornadiene Derivatives Using Magnesium Anthracene. J. Am. Chem. Soc. **2012**, 134, 13978–13981.
- Cowley, A. H. Terminal Phosphinidene and Heavier Congeneric Complexes. The Quest Is Over. Acc. Chem. Res. 1997, 30, 445-
- Groom, C. R.; Bruno, I. J.; Lightfoot, M. P.; Ward, S. C. The Cambridge Structural Database. Acta Cryst. B 2016, 72, 171-
- Pyykkö, P.; Atsumi, M. Molecular Double-Bond Covalent Radii for Elements Li-E112. Chem. Eur. J. 2009, 15, 12770-12779.
- Velian, A.; Nava, M.; Temprado, M.; Zhou, Y.; Field, R. W.; Cummins, C. C. A Retro Diels–Alder Route to Diphosphorus Chemistry: Molecular Precursor Synthesis, Kinetics of P_2 Transfer to 1,3-Dienes, and Detection of P₂ by Molecular Beam Mass Spectrometry. J. Am. Chem. Soc. **2014**, 136, 13586—
- Abbenseth, J.; Schneider, S. A Terminal Chlorophosphinidene
- Complex. Z. Anorg. Allg. Chem. 2020, 646, 565–569.
 Transue, W. J.; Nava, M.; Terban, M. W.; Yang, J.; Greenberg, M. W.; Wu, G.; Foreman, E. S.; Mustoe, C. L.; Kennepohl, P.; Owen, J. S.; Billinge, S. J. L.; Kulik, H. J.; Cummins, C. C. Anthracene as a Launchpad for a Phosphinidene Sulfide and for Generation of a Phosphorus-Sulfur Material Having the Composition P₂S, a Vulcanized Red Phosphorus That Is Yellow. J. Am. Chem. Soc. **2019**, 141, 431–440. Wellnitz, T.; Hering-Junghans, C. Synthesis and Reactivity of Monocyclic Homoleptic Oligophosphanes. Eur. J.
- Inorg. Chem. 2021, 2021, 8-21, eprint: https://chemistryeurope.onlinelibrary.wiley.com/doi/pdf/10.1002/ejic.202000878.
- (29) Transue, W. J.; Yang, J.; Nava, M.; Sergeyev, I. V.; Barnum, T. J.; McCarthy, M. C.; Cummins, C. C. Synthetic and Spectroscopic Investigations Enabled by Modular Synthesis of Molecular Phosphaalkyne Precursors. J. Am. Chem. Soc. 2018, 140, 17985-17991.
- (30) Zilm, K. W.; Webb, G. G.; Cowley, A. H.; Pakulski, M.; Orendt, A. The nature of the phosphorus–phosphorus double bond as studied by solid-state NMR. J. Am. Chem. Soc. 1988, 110, 2032-2038.
- (31) Duchamp, J. C.; Pakulski, M.; Cowley, A. H.; Zilm, K. W. Nature of the carbon-phosphorus double bond and the carbon–phosphorus triple bond as studied by solid-state NMR. J.
- Am. Chem. Soc. 1990, 112, 6803–6809. Gudat, D.; Hoffbauer, W.; Niecke, E.; Schoeller, W. W.; Fleischer, U.; Kutzelnigg, W. Phosphorus-31 Solid-State NMR Study of Iminophosphines: Influence of Electronic Structure and Configuration of the Double Bond on Phosphorus Shielding. J. Am.

- Chem. Soc. 1994, 116, 7325–7331. Geiß, D.; Arz, M. I.; Straßmann, M.; Schnakenburg, G.; Filippou, A. C. SiP Double Bonds: Experimental and Theoretical Study of an NHC-Stabilized Phosphasilenylidene. Angew. Chem. 2015, 127, 2777–2782.
 (34) Bohmann, J. A.; Weinhold, F.; Farrar, T. C. Natural chemical
- shielding analysis of nuclear magnetic resonance shielding tensors from gauge-including atomic orbital calculations. J. Chem.
- sors from gauge-including atomic orbital calculations. J. Chem. Phys. 1997, 107, 1173-1184.
 (35) Glendening, E. D.; Badenhoop, J. K.; Reed, A. E.; Carpenter, J. E.; Bohmann, J. A.; Morales, C. M.; Landis, C. R.; Weinhold, F. NBO 6.0 (Theoretical Chemistry Institute, University of Wisconsin, Madison, 2013).
 (36) Pinter, B.; Smith, K. T.; Kamitani, M.; Zolnhofer, E. M.; Tran, B. L.; Fortier, S.; Pink, M.; Wu, G.; Manor, B. C.; Meyer, K.; Baik, M.-H.; Mindiola, D. J. Cyclo-P3 Complexes of Vanadium: Reday Properties and Origin of the ³¹P NMR.
- of Vanadium: Redox Properties and Origin of the $^{31}\mathrm{P}$ NMR
- Chemical Shift. J. Am. Chem. Soc. **2015**, 137, 15247–15261. (37) Zhu, J.; Lau, J. Y. C.; Wu, G. A Solid-State ¹⁷O NMR Study of L-Tyrosine in Different Ionization States: Implications for Probing Tyrosine Side Chains in Proteins. J. Phys. Chem. B **2010**, *114*, 11681–11688.
- (38) Kong, X.; Terskikh, V.; Toubaei, A.; Wu, G. A solid-state ¹⁷O
- NMR study of platinum-carboxylate complexes: carboplatin and oxaliplatin. Can. J. Chem. 2015, 93, 945–953.

 Geeson, M. B.; Transue, W. J.; Cummins, C. C. Organoironand Fluoride-Catalyzed Phosphinidene Transfer to Styrenic Olefins in a Stereoselective Synthesis of Unprotected Phosphiranes. J. Am. Chem. Soc. 2019, 141, 13336-13340.

TOC graphic:



TOC Synopsis Anthracene-based phosphinidene transfer reagents react with a ruthenium $\operatorname{calix}[4]$ pyrrole complex to make a series of ruthenium(IV) phosphinidene complexes. Electronic structures of the phosphinidene complexes were interrogated using 31 P solid-state nuclear magnetic spectroscopy, which in conjunction with quantum chemical methods is a sensitive probe of metal-phosphorus multiple bonds.